

Numerical Modeling of the Evolution of Pore Water Pressure Within Cemented Paste Backfill Structure

Mamadou Fall and Liang Cui

Department of Civil Engineering, University of Ottawa, Ottawa, Canada

ABSTRACT

The pore water pressure (PWP) has a significant effect on effective stress and strength development in cemented paste backfill (CPB) structures. Moreover, the PWP has a considerable impact on stability and design of barricades. Hence, it has paramount and practical importance for stability analysis as well as the cost-effective design of CPB structures and barricades. In this study, a multiphysics model is developed and successfully validated against laboratory and field data to assess and predict the development and evolution of PWP within CPB mass. A series of engineering issues are then examined with the model to investigate the PWP in field CPB mass with respect to the changes in the mixture recipe, as well as the backfilling, surrounding rock and curing conditions. The obtained results provide in-depth insight into the PWP evolution in CPB.

INTRODUCTION

Cemented paste backfill (CPB) is extensively and increasingly used in mining operations for underground mine support, the maximization of ore recovery, and tailings waste management (Grice, 2001; Sivakugan et al. 2005). Once placed, the CPB structures as well as the barricades have to satisfy certain dynamic and static loading requirements to ensure a safe underground working environment for all mining personnel. Therefore, the mechanical stability of CPB and of barricades is an important design criteria of the CPB system.

The development of positive or negative pore water pressure (capillary pressure or suction) has a significant effect on the strength development and stability of CPB structures as well as on the stability of barricades. Moreover, the early development of capillary pressure in the CPB is also especially important for achieving early mechanical stability of the CPB (Li and Fall, 2016) as well as for the opening of the barricades. Thus, this will reduce the mining cycle and increase production, i.e., increase the profitability of the mine. Indeed, the critical challenge is to estimate the loads exerted onto the barricades and manage their opening time. These two issues are strongly influenced by the pore water pressure that develops behind the barricade, and suction development due to cement hydration. The latter results in the dissipation of excess pore pressure and increase in effective stress (i.e., strength gain) concurrent with transitioning from the paste phase to the hardening stage. This means the understanding and evaluation of (negative, positive) pore water pressure development and distribution in the CPB mass is critical for a cost-effective design of CPB structures and barricades (Li and Fall, 2016).

However, pore water pressure development in CTB structures is complex, since it is a function of the multiphysics or coupled (i.e., thermal (T; e.g., cement hydration heat; deep mine temperature), hydraulic (H; e.g., drainage, fluid flow), mechanical (M; e.g., stress; consolidation; deformation; filling rate), and chemical (C; cement reaction; mixing water chemistry; tailings chemistry and mineralogy);

THMC) processes that occur in CPB and thus control its behavior and performance (Cui and Fall, 2015). These complex and varying coupled THMC processes create their own special challenges for the adequate evaluation of the PWP development and distribution within a CPB structure, thus for the design of stable and cost-effective CPB structures. Thus, a reliable assessment of the development of positive and negative PWP in CPB mass absolutely requires the integration of these coupled THMC processes. However, at the time of writing, there is no model or modelling study that considers these multiphysics THMC processes in the assessment of the (negative and positive) PWP development in CTB structures. This research gap has resulted in the current modelling study, in which a multiphysics model for the prediction and assessment of PWP development in CTB is developed. Subsequently, the model is validated against both experimental data and in-situ measurements. Then, the model is used to understand and assess the pore pressure development in CPB for various practical cases or scenarios.

The main steps of the development and some validation results of the model as well as its application to simulate some practical problems in backfill operations are presented in this paper.

MODEL DEVELOPMENT

Modelling Approach

CPB is considered as a multiphase porous medium which consists of liquid (capillary water and physically adsorbed water), gaseous (pore air) and solid (binder, tailings and hydration products) phases. Moreover, once placed into a stope, a series of strong interactions between the coupled THMC processes immediately occur within the CPB structure. Therefore, the main THMC processes illustrated in Figure 1 are taken into consideration in the model development. The interaction between the coupling processes dominates the evolution of the material properties and behavior of the CPB structure (Cui and Fall, 2015). The main conservation and constitutive equations of the model are described in the next sections, whereas the determination of the model coefficients is presented elsewhere (Cui and Fall, 2015).

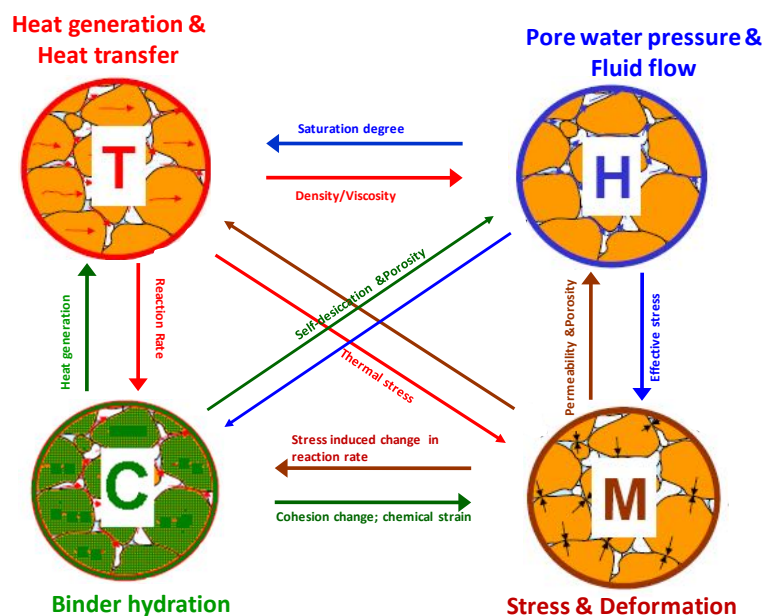


Figure 1. Main coupled THMC processes considered in the development of the multiphysics model

Main conservation Equations of the Multiphysics Model

The pore-water mass balance equation is expressed as:

$$n\rho_w \frac{\partial S}{\partial t} + nS \frac{\partial \rho_w}{\partial t} + S\rho_w \frac{\partial n}{\partial t} + \nabla \cdot (nS\rho_w \mathbf{v}^{rw}) = -nS\dot{m}_{hydr} \quad (1)$$

where ρ_w is the water density, n denotes the porosity, S refers to the degree of saturation, \mathbf{v}^{rw} indicates the relative apparent velocity of the pore water with respect to the solid phase velocity \mathbf{v}_s , and \dot{m}_{hydr} is the rate of water consumption per unit volume in the liquid phase due to binder hydration.

The energy balance equation is written as follows:

$$\begin{aligned} & \left[(1-n)\rho_s C_s + nS\rho_w C_w + n(1-S)\rho_a C_a \right] \frac{\partial T}{\partial t} + (\rho_w C_w \mathbf{v}^{rw} + \rho_a C_a \mathbf{v}^{ra}) \cdot \nabla T \\ & - \nabla \cdot (k_{eff} \nabla T) = Q_{hydr} \end{aligned} \quad (2)$$

where C_i refers to the specific heat capacity (i : air, water and solid phase), \mathbf{v}^{rw} and \mathbf{v}^{ra} denotes the fluid Darcy velocity, k_{eff} is the effective thermal conductivity of the CTB, and Q_{hydr} denotes the heat produced by the binder hydration.

The fully coupled multiphysics consolidation model detailed in Cui and Fall (2016) is used in this study.

$$\begin{aligned} & \left\{ [SP_w + (1-S)P_a] \frac{1-2\nu}{E} \frac{\partial \alpha_{Biot}}{\partial \xi} - \left\{ \frac{\sigma + \alpha_{Biot} [SP_w + (1-S)P_a]}{E} \right\} \left\{ \frac{9[1-2\nu]}{E} \frac{\partial E}{\partial \xi} + 18 \frac{\partial \nu}{\partial \xi} \right\} \right. \\ & - \alpha_{Biot} (P_a - P_w) \frac{1-2\nu}{E} \left\{ [1-S_e(P_w, P_a, \xi)] \frac{\partial \theta_r}{\partial \xi} + (n-\theta_r) \frac{\partial S_e}{\partial \xi} \right\} - \frac{(v_n + v_{ab-w})R_{n-w/hc}/(1-n)}{(w/c)v_w + v_c + (1/C_m - 1)v_{tailings}} - \frac{n\alpha_c}{1-n} \left. \right\} \frac{\partial \xi}{\partial t} \\ & + \frac{1-2\nu}{E} \frac{\partial \sigma}{\partial t} + \alpha_{Biot} \frac{1-2\nu}{E} \left\{ S - (P_a - P_w)(n-\theta_r) \frac{\partial S_e}{\partial P_w} \right\} \frac{\partial P_w}{\partial t} + \frac{\partial \lambda}{\partial t} \frac{\partial g_{CTB}}{\partial I_1} + \alpha_{Ts} \frac{\partial T}{\partial t} \\ & + \alpha_{Biot} \frac{1-2\nu}{E} \left\{ (1-S) - (P_a - P_w)(n-\theta_r) \frac{\partial S_e}{\partial P_a} \right\} \frac{\partial P_a}{\partial t} \\ & = - \left\{ (1-n) + \alpha_{Biot} (P_a - P_w) \frac{1-2\nu}{n^2 E} [n(1-n)S_e + (1-S_e)\theta_r] \right\} \frac{\partial n}{\partial t} \end{aligned} \quad (3)$$

where P_w and P_a respectively denote the pore-water and pore-air pressure, S_e is the effective degree of saturation, α_{Biot} is the Biot's effective stress coefficient, E and ν denote the elastic modulus and Poisson's ratio, respectively, ξ is the degree of binder hydration, θ_r is the residual water content, v_w , v_n , v_{ab-w} , v_c and $v_{tailings}$ respectively stand for the specific volume of the capillary water, chemically combined water, physically absorbed water, cement and tailings, C_m is the binder content, w/c represents the water to cement ratio, $R_{n-w/hc}$ is the mass ratio of the chemically combined water and hydrated cement, λ is a non-negative plastic multiplier and g_{CTB} is a plastic potential function, and α_{Ts} is the coefficient of the thermal expansion (CTE) of the solid phase of the CTB.

The pore-air mass balance equation is expressed as follows:

$$n(1-S) \frac{\partial \rho_a}{\partial t} - n\rho_a \frac{\partial S}{\partial t} + (1-S)\rho_a \frac{\partial n}{\partial t} + \nabla \cdot \phi(1-S)\rho_a \mathbf{v}^{ra} = 0 \quad (4)$$

Constitutive Relations

Water retention model. The modified van Genuchten model (Al-Hussain and Fall, 2011) is used in this study to simulate the time-dependent water retention curve (WRC) of CPB. The model is expressed as

$$\theta = \theta_r + \frac{(\theta_s - \theta_r)}{\left[1 + (\alpha_{wrc} P_c)^{n_{wrc}}\right]^{m_{wrc}}} \quad (5)$$

where α_{wrc} , n_{wrc} and m_{wrc} are three different model parameters and change with the binder hydration, n_{wrc} is related to m_{wrc} through $n_{wrc} = 1/(1 - m_{wrc})$, θ_s refers to the saturated water content and equals the CTB porosity \mathcal{N} , and θ_r is the residual water content.

Pore fluid flow model. Darcy's law is used to describe the fluid flow for liquid water \mathbf{v}^{rw} and dry air \mathbf{v}^{ra} :

$$\mathbf{v}^{ri} = -K \frac{k_{ri}}{\rho_i g} \nabla (P_i - \rho_i g) \quad (6)$$

where K refers to the saturated hydraulic conductivity, k_{ri} denotes the relative permeability with respect to each fluid, μ_i stands for the fluid dynamic viscosity, and P_i denotes the pore fluid pressure. The hydraulic conductivity K is related to the viscosity pore fluid and the CTB porosity. Due to the development of consolidation in the CTB, the variation of the porosity will result in changes in K . Detailed information on determining the hydraulic conductivity is Cui and Fall (2015).

Degree of binder hydration model. The model proposed by Schindler and Folliard (2005) is applied to predict the progression of binder hydration, which has been successfully applied to CTB materials in previous studies.

$$\xi(t_e) = \left(\frac{1.031 \cdot w/c}{0.194 + w/c} + 0.5 \cdot X_{FA} + 0.30 \cdot X_{slag} \right) \exp \left[- \left(\frac{\tau}{t_e} \right)^\beta \right] \quad (7)$$

$$\text{with } \begin{cases} t_e = \sum_0^t \exp \left[- \frac{E_a}{R} \left(\frac{1}{T} - \frac{1}{T_r} \right) \right] \cdot \Delta t \\ E_a(T) = \begin{cases} 33,500 + 1,470(20 - T) & T < 20^\circ C \\ 33,500 & T \geq 20^\circ C \end{cases} \end{cases}$$

where w/c denotes the water to cement ratio, X_{FA} and X_{slag} respectively stands for the weight fraction of the fly ash and blast furnace slag relative to the total binder weight, τ and β respectively refer to the hydration time (hours) and shape parameters, t_e is the equivalent age at the reference temperature T_r , E_a is the activation energy (J/mol), and R is the universal gas constant (8.314 J/mol/K). The degree of binder hydration model (Equation 7) can be used to determine the pore water sink terms \dot{m}_{hydr} in Equation (1) and heat source term Q_{hydr} in Equation (2) as detailed in Cui and Fall (2015, 2016).

MODEL VALIDATION

The multiphysics model presented above was first implemented into a finite element method (FEM) code, COMSOL Multiphysics. Then, five case studies were used to test the capabilities of the developed model to describe and predict the pore pressure development and distribution within CPB mass. The case studies cover both laboratory experiments (performed in this study and in other studies) and field measurements. The validation results have shown good agreement between the predicted and experimental results. An example of results of validation against field measurements is presented below, whereas other examples are given in Cui and Fall (2015, 2016).

A field monitoring program conducted by Yumlu (2008) in the Çayeli mine is selected for this validation example. In this monitoring program, a piezometer (model: Geokon 4500S) was installed on a rigid instrument frame to record the changes of the PWP in the stope environment. The monitored point was located 0.5 m from the stope floor along the centerline of the stope. Detailed information on the monitoring program (i.e., the binder recipe, backfilling strategy, and initial and boundary conditions) is provided in Cui and Fall (2015, 2015). In terms of the simulation, the modelled geometry, the sensor location, mesh grid and monitoring point are presented in Figure 2.

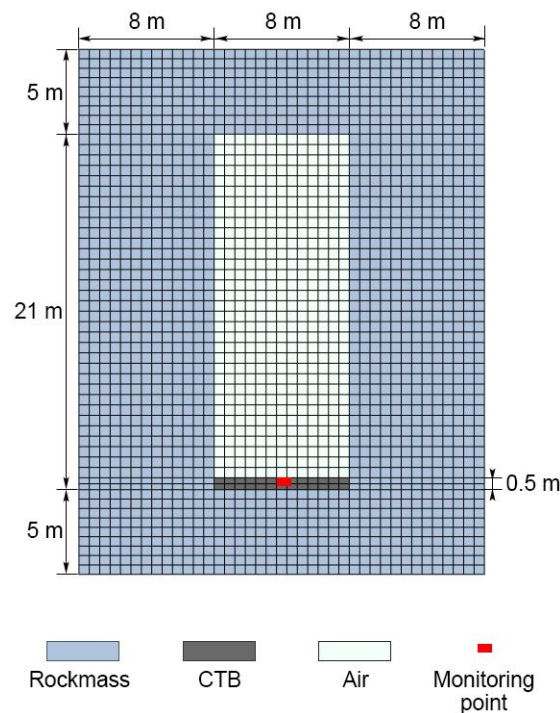


Figure 2. Modelled geometry, mesh and monitoring point for the selected field case

The changes in the PWP and filling process in three stages are plotted in Figure 3. It can be seen that the PWP increases immediately after fresh CTB is placed into the stope. After completion of the first stage of filling, the PWP shows a decreasing trend during the first curing. Afterwards, even though fresh CTB is poured into the stope for the following stages of filling, no apparent increase in PWP is observed. As shown in Figure 3, the trend and changes in PWP are adequately captured by the model.

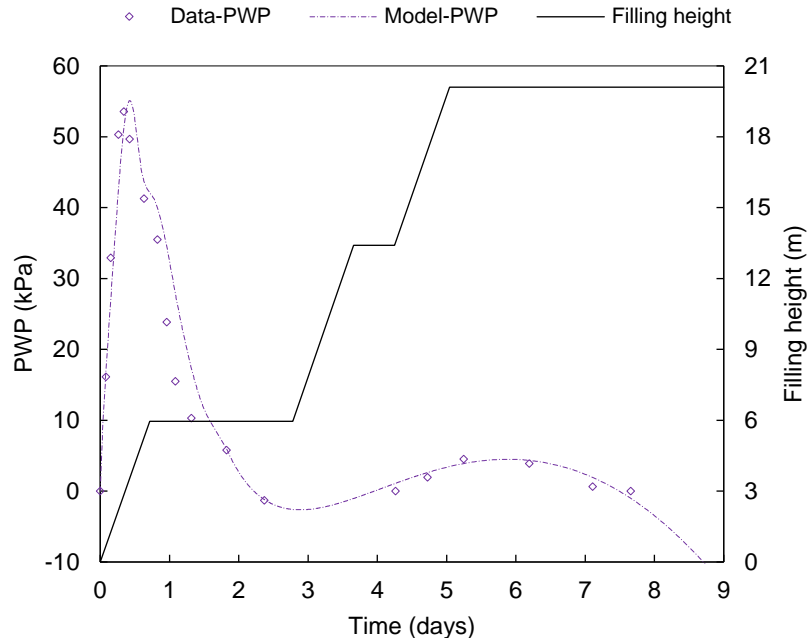


Figure 3. Comparison between numerical prediction results and experimental data for PWP

NUMERICAL SIMULATION RESULTS

After the validation of the developed model with different case studies, the model was applied to simulate the development and distribution of PWP (positive, negative) in CPB structures in various conditions or influencing factors. The factors were selected to study the effect of curing time, stope geometry (size, shape, angle and height), mixture recipe, initial CPB and rock temperatures, binder content, and backfilling rate and strategy (presence vs absence of plug, curing time of the plug) on the PWP development and distribution in CPB structures. Valuable results were obtained with regards to the PWP response of CPB structures. Some samples of simulation results are presented and discussed below. To assess the impacts of these factors, a control CTB mass was used as the reference for the model application. The mixture recipe, backfilling conditions, initial and boundary conditions of the control CTB, and the geometry and mesh of the control CTB mass and stope are given in Cui and Fall (2016). To evaluate the PWP changes in the CTB, a monitoring point located at 0.1 m from the floor of the stope is examined.

Time-Dependent Evolution of the PWP in a CPB Structure

The PWP change in CTB with curing time for the selected stope is plotted in Figure 4. It can be observed that the positive PWP increases with time at the very beginning of the first backfilling stage. The positive PWP gradually increases with CPB depth at a curing age of 0.5 day (i.e., during the 1st filling stage). After the completion of 1st stage backfilling, CPB will be allowed to cure for 50 h. During the curing time, the negative PWP pressure appears at the top domain of CPB as shown in Figure 4(b). The generation of negative PWP can be attributed to the water consumption by binder hydration and fluid migration under gravity effect within CPB. Afterwards, although the 2nd-stage backfilling is carried out, the majority of CPB domain is affected by the negative PWP (e.g., at the age of 96 h or 4 days, Figure 4(c)). As expected, positive PWP is generated on the top domain of CPB at the 3rd stage of backfilling (Figure 4(d)) due to the placement of fresh paste into the stope.

Therefore, the obtained results indicate that curing time can significantly affect the PWP in CTB. With curing time, the PWP is progressively dissipated in the CTB resultant of the water consumption due to binder hydration. However, there is a limit to the pore-water consumption due to binder hydration.

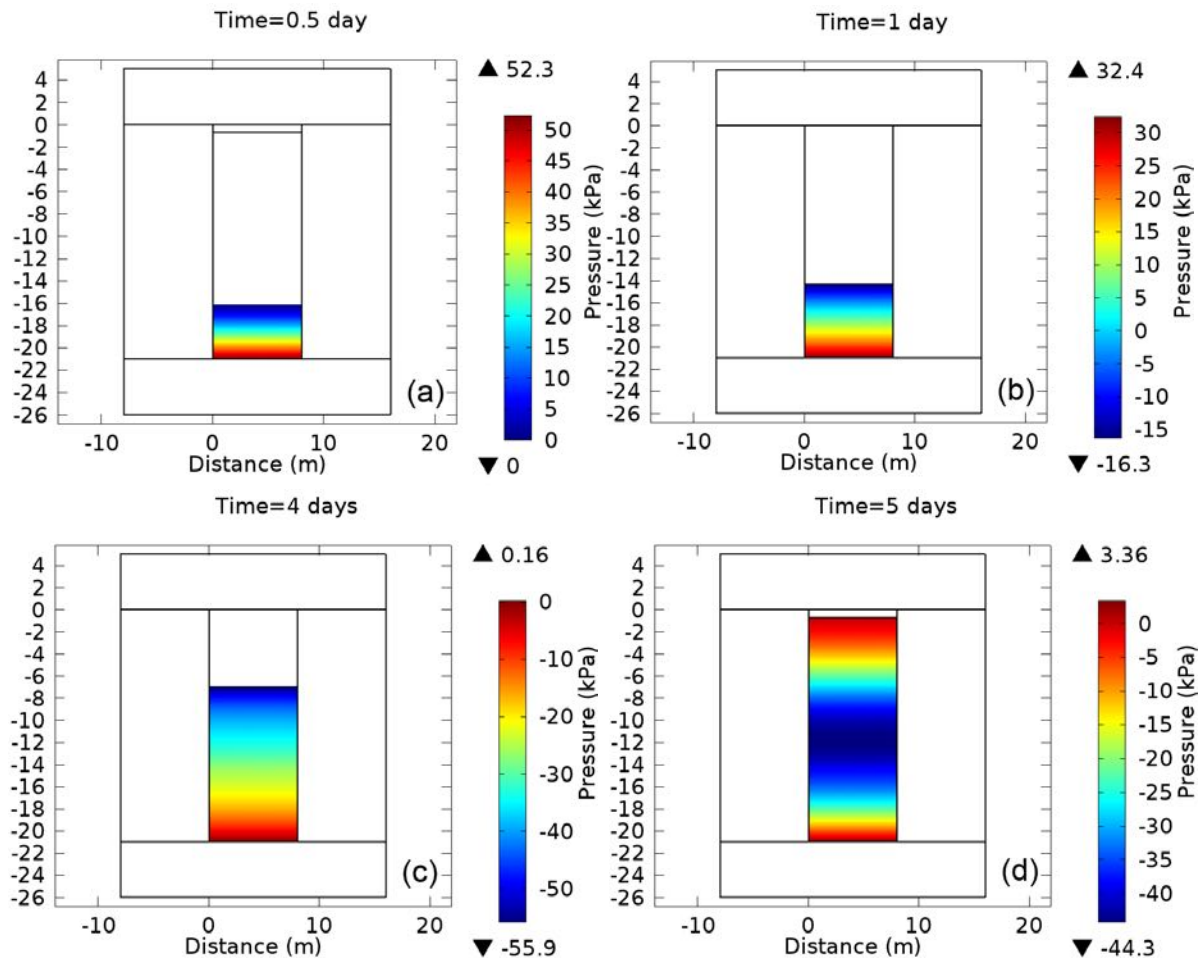


Figure 4. Simulated evolution of spatial distribution of pore water pressure for different curing time: (a) 0.5 day; (b) 1 days; (c) 4 days; (d) 5 days

Effect of Initial Backfill Temperature on the Evolution and Distribution PWP in a CPB Structure

Since CPB is a mixture of binders, water and tailings, its initial temperature is strongly affected by the initial temperatures of tailings and water. In addition, when preparing CPB, moderate heat could be added to achieve a high early strength within its Fall et al. 2007). Furthermore, the increase of the temperature in fresh backfill can occur during its transport in pipes from the surface to the underground working areas of a production section (Fall et al. 2010). These variable initial temperatures of fresh CPB make it necessary to investigate the effect of initial CPB temperatures on the heat developed within the CPB. To study the impact of the initial temperature in the CTB, the temperature of the fresh CPB placed in the control stope was 5°C, 25°C and 45°C, respectively. As shown in Figure 5, the PWP will dissipate to a greater extent with a higher initial temperature. The obtained results indicate that the initial temperature of the CPB has a significant influence on PWP, and thus the trend and changes in PWP.

Therefore, under a higher initial temperature, lower PWP and thus higher effective stress can be obtained more rapidly, which is favorable for the stability of CTB structures and barricades.

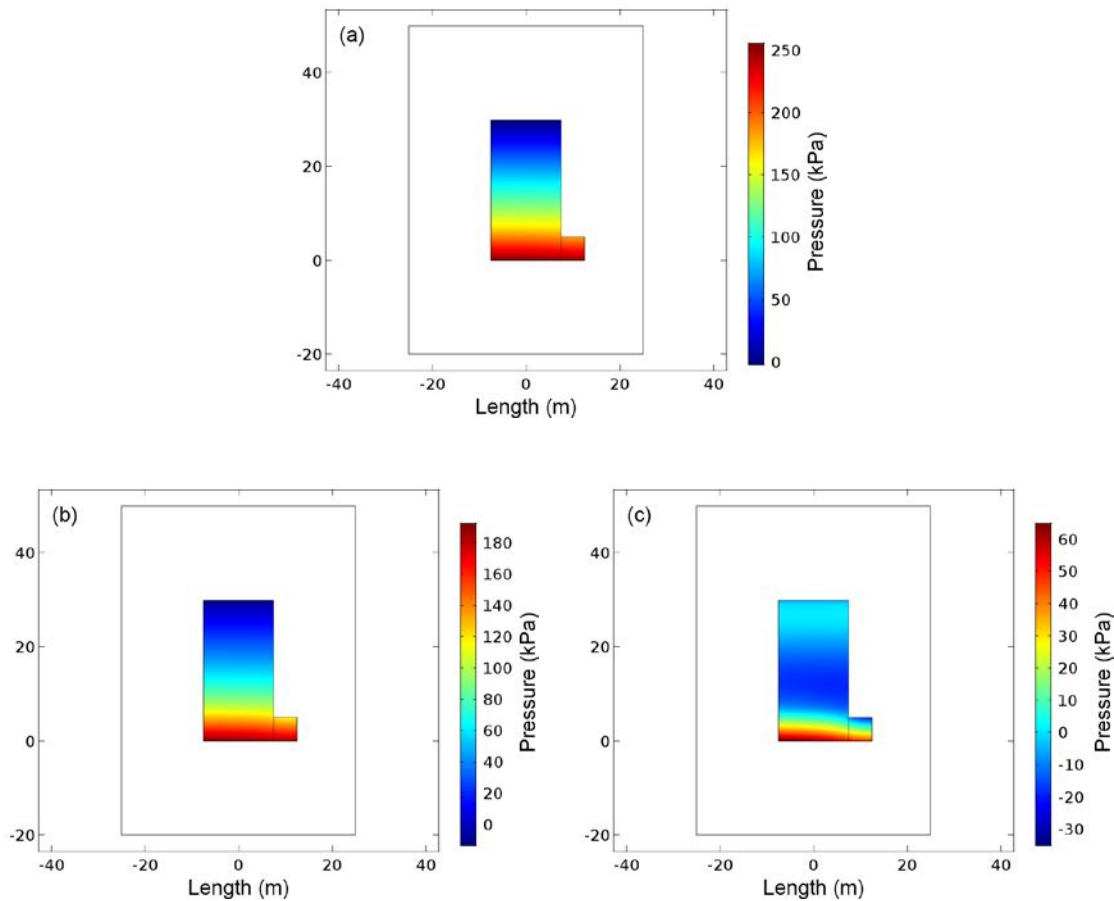


Figure 5. Spatial distribution of PWP in CTB with different initial temperatures at the completion of backfilling (3.5 days): (a) 5°C; (b) 25°C; and (c) 45°C

Effect of Binder Content on the Evolution and Distribution PWP in a CPB Structure

Binder content is a significant factor that influences the strength and cost of CPB; therefore, it is crucial to obtain an appropriate binder content to fulfill both the mechanical stability of the CPB and decrease its cost. The binder content has the most significant effect on the cost of CPB. In this study, three different cement contents, including 1 wt% (16.7 kg/m³), 4.5 wt% (75.3 kg/m³), and 7 wt% (117.1 kg/m³) (wt%: weight percentage of cement with respect to the total weight of solid phase in CTB) are examined to investigate their impacts on PWP in the selected stope. The changes in the PWP in CPB with the different cement contents are plotted in Figure 6. It is evident that obvious changes in the PWP start from the first day of curing. As the backfilling progresses, it can be seen that the PWP is significantly reduced in the CPB with a higher cement content. For instance, the PWP peak with a cement content of 7 wt% is reduced by 46% (i.e., from 272 kPa to 147 kPa) in comparison to the case with a cement content of 1 wt%. Moreover, the PWP peak appears before the completion of backfilling for the case with a cement content of 7 wt%; namely, water consumption due to hydration with higher cement contents can counteract the effect of fresh CTB placement. This is because a higher cement content will mean the consumption of more

capillary water at same filling rate and/or at the same curing time. Consequently, lower PWP is obtained in the CTB with a higher cement content.

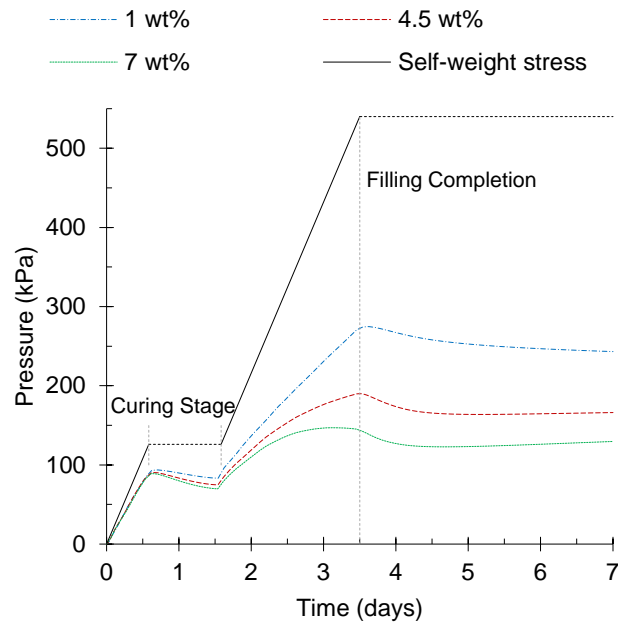


Figure 6. PWP changes in CTB with different cement contents

CONCLUSIONS

The following conclusions are made based on the obtained results.

- (i) A multiphysics model is developed and successfully validated to predict the PWP development and distribution in CTB structure. The proposed model fully considers the coupled THMC processes that occur in CTB.
- (ii) The developed model is used to examine a series of engineering issues, including the effect of the curing time, binder content, stope geometry, mixture recipe, backfilling rate and strategy, and the initial temperature of the CTB and rock mass.
- (iii) The simulation results show that these issues affect the PWP development and distribution in CPB mass to different extents.
- (iv) This developed multiphysics tool and the simulation results have the potential to assess and provide an understanding of the PWP in hydrating CTB mass in field loading conditions, and thus contribute to the design of cost-effective CPB structures and barricades.

REFERENCES

- Abdul-Hussian, N., and Fall, M., 2011. Unsaturated hydraulic properties of cemented tailings backfill that contains sodium silicate. *Engineering Geology*, 123(4): 288-301.
- Cui, L., Fall, M. (2016). Multiphysics model for consolidation behaviour of cemented paste backfill. *ACSE International Journal of Geomechanics* (in press).
- Cui, L., Fall, M. (2015). A coupled thermo-hydro-mechanical-chemical model for underground cemented paste backfill. *Tunnelling and Underground Space technology* 50:396-414.

- Fall, M., Nasir, O., and Celestin, J.C., 2007. Paste backfill responses in deep mine temperature conditions. *In 9th International Symposium of mining with backfill*. Montreal, Canada, CD-Rom.
- Li, W., Fall, M. (2016). Sulphate effect on the early age strength and self-desiccation of cemented paste backfill. *Journal of Construction and Building Materials* 106: 296-304.
- Fall, M., Celestin, J.C., Pokharel, M., and Touré, M., 2010. A contribution to understanding the effects of curing temperature on the mechanical properties of mine cemented tailings backfill. *Engineering Geology*, 114(3-4): 397-413.
- Grice T. Recent mine developments in Australia. *Proceeding of the 7th international symposium on mining with backfill (MINEFILL) 2001*; 351-7.
- Schindler, A.K., and Folliard, K.J., 2005. Heat of hydration models for cementitious materials. *ACI Materials Journal*, 102(1): 24-33.
- Sivakugan, N., Rankine, K.J., and Rankin, K.S., 2005. Geotechnical consideration in mine backfilling in Australia. *Journal of Cleaner Production*, 14(12-13): 1168-1175.
- van Genuchten, M.T.H., 1980. A closed-form equation for predicting the hydraulic conductivity of unsaturated soils. *Soil Science Society of America Journal*, 44(5): 892-898.
- Yumlu, M., 2008. Barricade pressure monitoring in paste backfill. *Gospod. Surowcami Min.* 24, 233-244.